University of San Carlos
Department of Chemical Engineering

CHE 3214L Chemical Engineering Laboratory Investigations 1

Data Processing & Analysis Report

(Form CHE 3214L-3)

Prepared and submitted by:

Chillann Kirk D. Illaga | Jerold J. Monsanto | Jean Mercy C. Rosal

Experiment 4: **Hydrodynamics in a Packed Absorption Column**

Objectives of the Experiment

1. Determine experimentally the pressure drop across a wet column as a function of the air flow rate and compare the results with theoretically calculated values.
2. Determine through visual observation and by graphical methods the loading and the flooding points of the packed column at pre-set values of water flow rates.
3. Construct from experimental data the loading and the flooding curves of the packed column based on the generalized correlations proposed by Sherwood, Shipley, and Holloway.

Results & Discussion

In the industry, packed towers are often used for separation procedures like absorption, stripping, and distillation. Absorption is a mass-transfer process in which a specific material enters a bulk phase, such as a vapor solute in a gas mixture entering a liquid mixture in which the solute is soluble. The packed tower operates in a countercurrent flow, with liquid entering from the top and exiting at the bottom, and gas entering from the bottom and exiting at the top. The tower packings, which must have a large surface area per volume, aid in good liquid-to-gas interaction.

The hydrodynamics of these packed absorption columns are investigated in order to determine the pressure drop across the column in order to estimate the power requirement as the column is operated, as well as to determine the loading, flooding, and channeling points at predetermined air and water flow rate values for operational purposes.

1. Pressure drop across a wet column as a function of air flow rate

Pressure drop across a packed absorption column is of importance since it is related to the safe operation of a plant. The pressure drop can be determined experimentally by measuring the difference in height of the fluid in the differential manometer as the gas passes along the column. It can be presented mathematically as

$$\Delta P_{exp} = \rho_L g \Delta h \qquad [1\text{-}1]$$

where ΔP_{exp} is the experimental pressure drop, Δh is the height difference reading in the manometer, ρ_L is the density of water at ambient temperature, and g is the gravitational constant. Two trials were conducted for this part of the experiment since manometer readings were taken when the air flow rate was increased and when the air flow was decreased.

The pressure drop in a packed column can also be calculated using a theoretical method like Ergun's equation which can be presented as

$$\Delta P_{theo} = \frac{150\ \mu v' \Delta L}{D_p^2}\frac{(1-\varepsilon)^2}{\varepsilon^3} + \frac{1.75\rho(v')^2\Delta L}{D_p}\frac{(1-\varepsilon)^2}{\varepsilon^3} \qquad [1\text{-}2]$$

where ΔP_{theo} is the theoretical pressure drop, μ is the fluid viscosity, v' is the fluid superficial velocity, ΔL is the length of the packed bed, D_p is the effective particle diameter, and ε is the porosity.

Ergun presented a general equation to calculate the pressure drop across a packed bed for all flow conditions using an extensive set of experimental data covering a wide range of particle size and shapes (Bayram et al., 2018). Shown in Equation 1-2 , it combines both the laminar and turbulent components of the pressure loss across a packed bed. The first term of the equation is for laminar flow conditions where the pressure drop through the packed bed is independent of the fluid density and has a linear relationship with superficial velocity. While for the turbulent flow, the second term of the equation, the pressure drop increases with the square of the superficial velocity and has a linear dependence on the density of the fluid passing through the bed (Geankoplis et al., 2018).

Table 1. Equipment specifications and fluid properties

Column	
Column Diameter (D_C), *m*	0.0175
Column Length (ΔL), *m*	0.595
Sampling points	S1 and S2
Packing	
Packing Material	Rachig rings
Packing Diameter (D_P), *m*	0.0027
Specific surface area (a_v), m^{-1}	420
Sphericity (ψ_s)	0.3
Porosity (ε)	0.63
Liquid	
Type of liquid	Water
Initial Temperature (T), °C	28
Final Temperature (T), °C	27
Viscosity (μ), *Pa·s*	0.000842
Density (ρ), $kg \cdot m^{-3}$	996.39
Gas	
Type of gas	Air
Initial Temperature (T), °C	26
Final Temperature (T), °C	29
Viscosity (μ), *Pa·s*	1.85×10^{-5}
Density (ρ), $kg \cdot m^{-3}$	1.174

Shown in the table above are the packed column data and setting which were required in the actual conduct of the experiment. In this experiment, the sampling points used were S1 and S2 which were the top and bottom portion of the absorption column, respectively. The column length was also accounted for however it is noted that the column length used in the calculations only accounted for the part of the column where there are Raschig rings packings since there were void spaces that had no packings seen at the top of the column. Sphericity was also determined since Ergun's equation was derived with the assumptions that the packings are spherical; however in this case, the packings were hollowed cylinders. Hence to minimize inconsistencies and errors, sphericity was used. The density and viscosity of water and air were taken from the book Transport Processes and Separation Process Principles (Geankoplis et al., 2018).

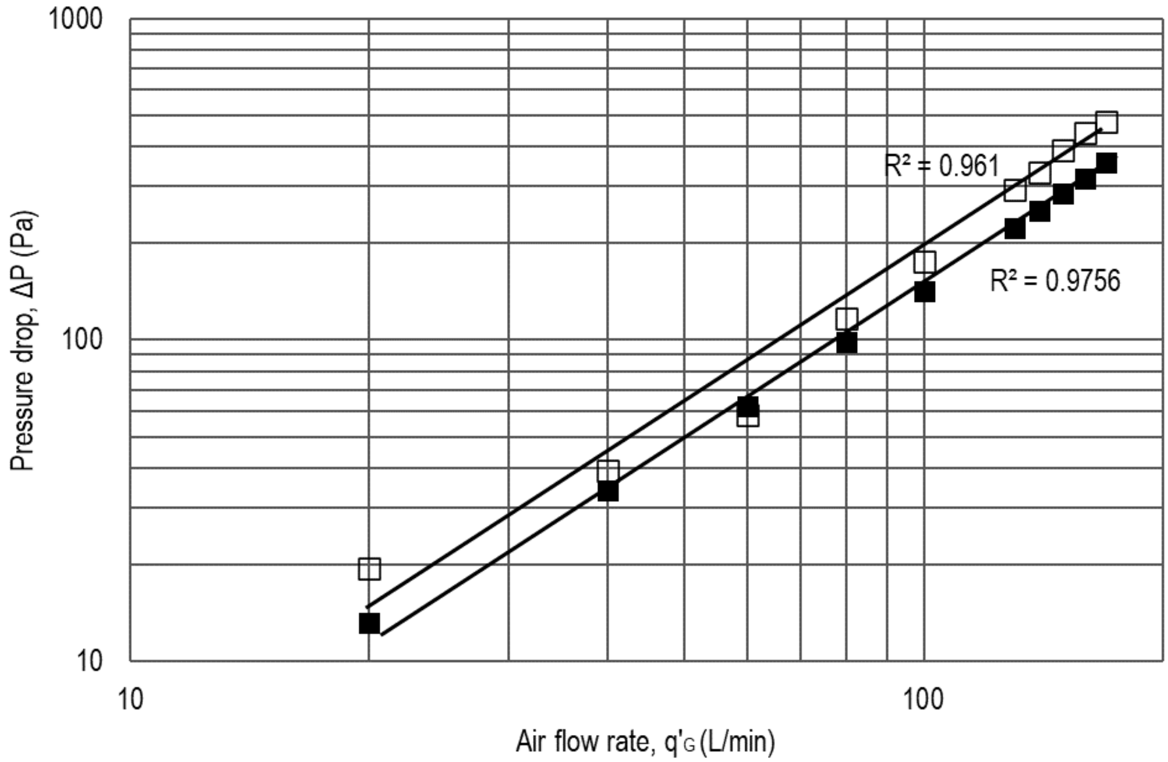

Figure 1.1. Pressure Drop Across a Wet Column as a Function of the Air Flow Rate across S1-S2 for Air-water system (solid symbol: theoretical; open symbol: experimental).

It can be observed from the graph that the pressure drop increases with increasing air flow rate. This can be justified by the values of the Pearson correlation coefficient of 0.961 and 0.9756 for both the experimental and theoretical values of the determined pressure drop respectively which is close to the value of $R^2 = 1$. It suggests that there is a strong correlation between air flow rate and pressure drop. For every positive increase in air flow rate, there is a positive increase in pressure drop. This is due to the fact that the pressure drop is proportional with the air velocity since it can be recalled that the volumetric flow rate is related to the fluid velocity. Fluid friction in the form of drag and skin friction causes pressure to build up at the bottom of the column, increasing the height difference in the water manometer. This shows that the pressure difference over the entire column has increased (McCabe et al., 2005). Moreover, the increase in the kinetic energy of the air molecules causes more interactions hence creating more opposing forces resulting in an increase in pressure drop. The value of the pressure drop is affected by the flow resistances in the system; more flow resistances equals a bigger pressure drop

Comparison between the pressure drop measured experimentally and the pressure drop calculated using the Ergun's equation is also shown in Figure 1.1. As the graph indicates, the theoretically calculated pressure drop at varying air flow rates is less than the experimentally measured pressure drop. One assumption of the Ergun's equation is that the packings are spherical while on the actual conduct of the experiment, the packings used were raschig rings. A sphericity factor which has a value of 0.3 was accounted for in the calculations. It can be inferred that this difference between the experimental and theoretical pressure drop is because there is a part of the column where there were no packings. The length that was accounted for during the calculations was only at the length where the packings are present. Hence, the pressure drop in the void space where there are no packings was unaccounted. Moreover, the wetness of the packings which resulted in the reducing of space the gas can pass through was not accounted for during the calculations for the theoretical pressure drop (McCabe et al., 2005). Also in theory, the pressure drop increases when the packed column is wet rather than dry. Other factors include inaccurate adjustment of flow rates by manual rotation of the air flow valve.

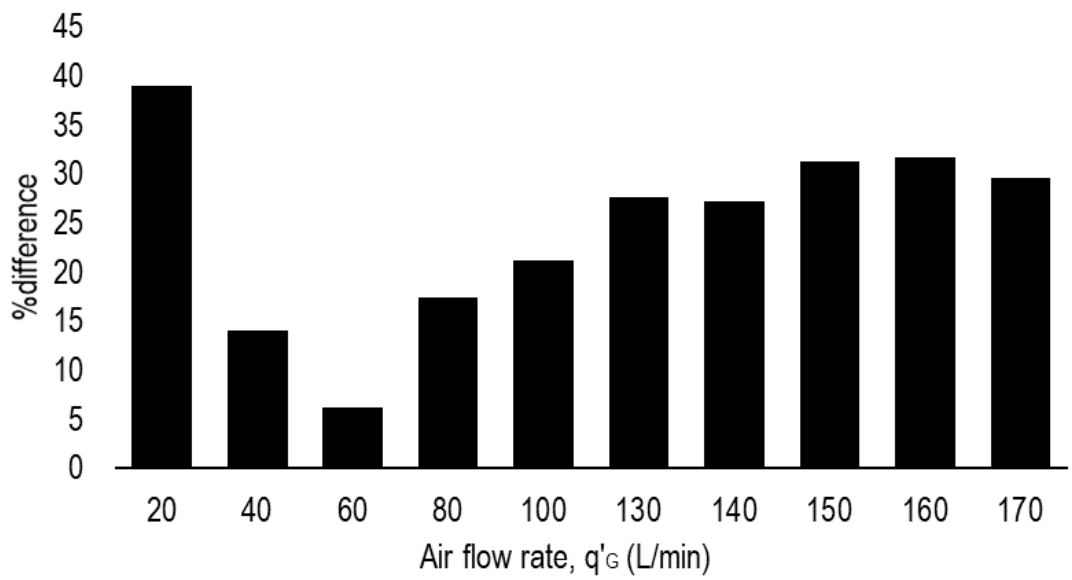

Figure 1.2 Percent Difference of Experimental and Theoretical Pressure Drop at Different Air Flow Rates.

The percent difference between the experimental and theoretical at different air flow rates ranges from 6-40% as shown in the figure above. It can be observed from the graph that there is a fluctuating percent difference between various air flow rates. These errors may have resulted due to the unaccounted factors such as the different friction losses due to a wet column or expansion at the air inlet. In the case of the wet packed column, the resistances to flow is offered by the drag force brought about by the packed bed, the skin friction of the tower and the additional drag force offered by the liquid in the packed column that is why the pressure drop is higher compared to that of the dry column where the resistances to flow is offered only by the packed bed and the skin friction (Coulson et al., 2002).

2. Loading and flooding points of the packed column at pre-set values of water flow rates

Packed absorption towers through which two fluids, in this case air and water, flowing in countercurrent enabling component/s to be transferred from one fluid phase to the other, are essential units in almost all chemical plants. One of the key aspects of the packings in a column is allowing an intimate contact as possible between the ascending gas and descending liquid. Hence, it is important to have an understanding and knowledge of both fluid flows and mass transfer in the plant operations given the significance of absorption columns. Like any other industrial processes, certain issues would arise in packed columns of which flooding is a major concern. Flooding is a phenomenon by which the liquid could no longer flow down through the packing. This is undesirable because it is accompanied by a dramatic rise in pressure drops across the columns resulting in detrimental consequences affecting the performance of the absorption process (Ajibola, 2010). The point where flooding occurs, or the flooding point is the upper limit by which the column must operate. On the other hand, a lower limit must also be identified. This is called the loading point in which the gas starts to hinder the liquid down flow, and local accumulations of liquid start to appear in the packing at the bottom of the column. Moreover, below the loading point there exists a phenomenon called channeling.This is also not desirable since the liquid will have the tendency to segregate towards the regions of the greatest void space and the walls of the packed column; hence, leads to low mass transfer efficiencies. Flow parameters and packed column settings are considered for the operation. This includes ten air flow rates at varying water flow rates shown in Table 2.1, sampling points, and types of fluid.

Table 2.1. Packed column settings and flow parameters

Manometer Type	Sampling Points	Water flow rates, q'_L (L/min)
Water	S1 and S2	1.5, 2.0, 2.5, 3.0, 3.5, 4.0, 4.5

In this experiment, the flooding and loading points are determined through visual and graphical methods. By visual observation, the flooding point can be identified when bubbles start to form at the top of the column which indicates that liquid is prevented from going down the column. Moreover, the loading point is identified when liquid starts to accumulate at the bottom of the column.

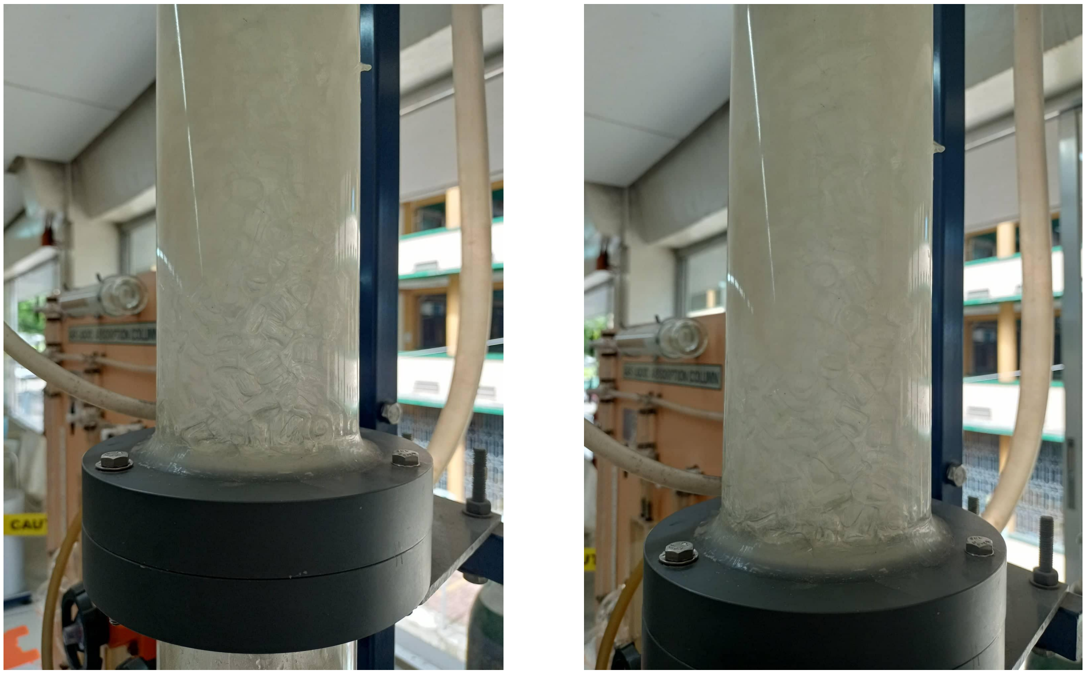

(a) no loading (b) loading point

Figure 2.1. Bottom of the column where (a) no loading occurs and (b) loading phenomenon occurs

Shown in figure 2.1-a is the illustration of the bottom part of the column in which no loading occurs. In this circumstance, at low gas and water velocities, the water would just pass flow through the column. However, when the gas velocity is increased, local pools of water start to appear in the packing as shown in figure 2.1-b. There is a liquid holdup that can be observed since the liquid is hindered by the air flow. At this instant, the liquid could not fall down the packing at the same rate as the applied feed rate.

(a) no flooding (b) flooding point

Figure 2.2. Top of the column where (a) no flooding occurs and (b) flooding phenomenon occurs

Shown in figure 2.2-a is the upper part of the column where no flooding occurs. However, when the gas velocity is increased after which the loading point can be observed, a point is reached at which the liquid overflows in the column. This is shown in figure 2.2-b wherein bubble formation can be seen. At this point, there is a tendency that the liquid and gas move out of the column since the accumulation of liquid becomes so high that it would be greater than that of the packing in the column.

For the second method, the loading points and flooding points are identified graphically using the plot of pressure drop per packed column length vs the gas mass velocity as shown in the figure below.

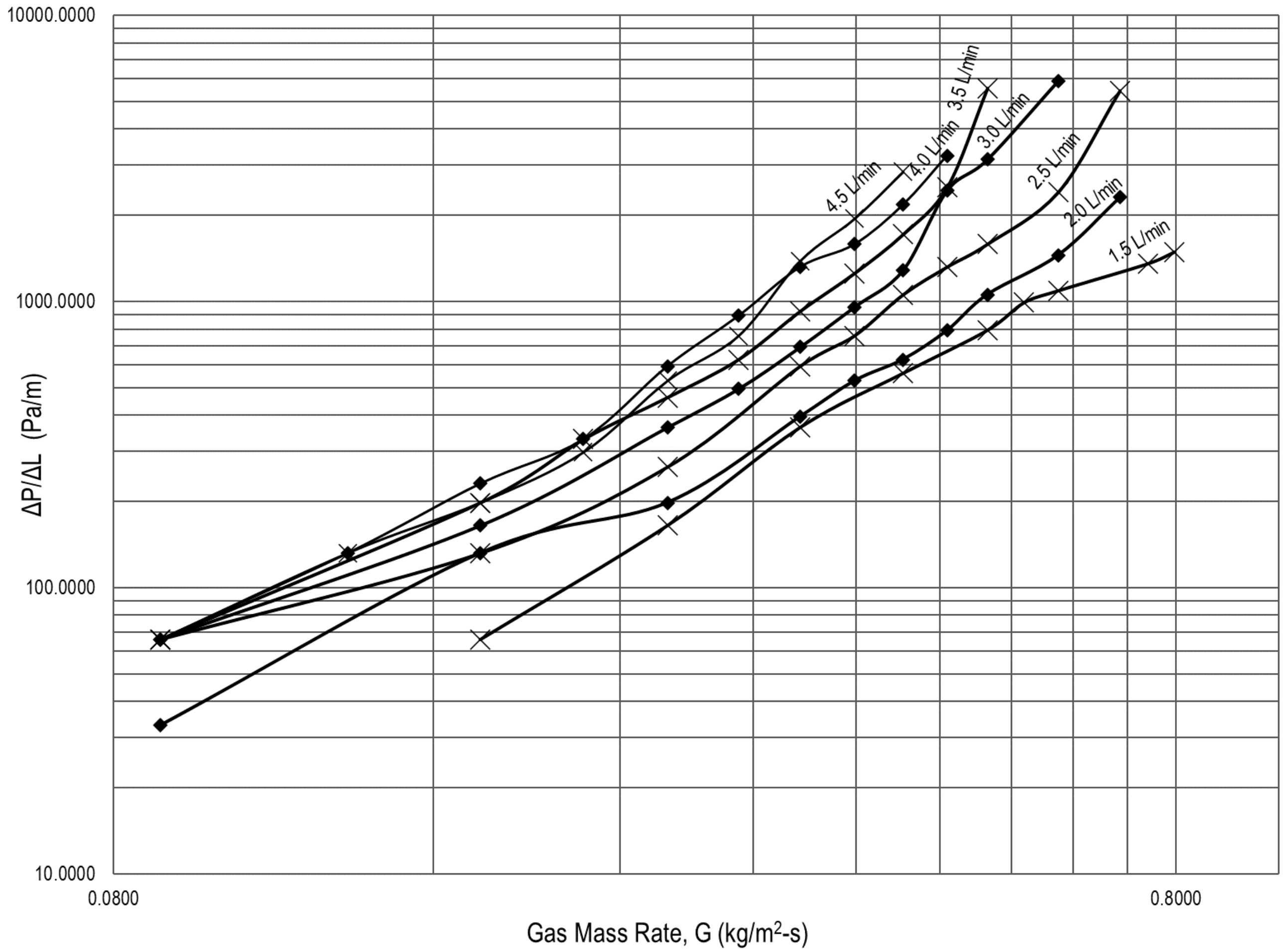

Figure 2.3. Pressure Drop as a Function of Gas Mass Rate, G in a Packed Column across S1-S2 for Air-Water System of Varying Water Flow Rates at T=30°C

The pressure drop in the column is dependent on both the gas and liquid flow rates, as shown in Figure 2.3, because a slight increase of either of the flow rates results in an increase in the pressure of the column. Moreover, as pressure drop increases, the slope at different water flow rates become steeper. This is because the gas is starting to impede the descending liquid and the liquid holdup increases with gas rate. Hence, there is an increase in drag force against the packing and falling water. It can also be observed that there are points where there is a significant rise in pressure drop as represented by a sudden change in slope.

The point at which the first sudden change in slope in the graph signifies the loading point. This is the start where the pressure drop between two points is greater than those before the loading point. The liquid accumulating on the column packing causes the pressure below the flooding point to increase.

Furthermore, the second change of slope wherein the lines become almost vertical signifies the flooding point (McCabe et al., 2005). Gradually increasing the gas flow rate after loading point is achieved, very large pressure drops would be recorded. Liquid starts to accumulate rapidly that the entire column would be filled with liquid. The forces that contribute to the pressure drop are the fluid friction and form drag. At higher velocities, form drag predominates (Foust, 1980). The flooding and loading points at varying water flow rates are tabulated below.

Table 2.2. Loading and Flooding Points of the Packed Column at Varied Water flow Rates Obtained Graphically and Visually

Water flow rate, q'_L (*L/min*)	Air flow rate, q'_G (*L/min*)			
	Loading points		Flooding points	
	Visual	Graphical	Visual	Graphical
1.5	-	-	-	-
2.0	160	140	-	-
2.5	140	120	160	160
3.0	120	100	140	140
3.5	100	110	120	120
4.0	90	80	110	110
4.5	80	70	90	100

Shown in table 2.2 are the loading and flooding points of the packed column at varied water flow rates which were determined by visual observation and graphical method. In the table, there were no loading and flooding points at a water flow rate of 1.5 L/min even at maximum air flow rate setting. For a water flow rate of 2.0 L/min, a loading point was observed at 160 L/min via visual observation and 140 L/min via graphical method. However, no flooding point was observed at this water flow rate. The first flooding point determined is at 2.5 L/min water flow rate. At slower water flow rates where no flooding occurred, the amount of air supplied by the equipment is not enough to cause flooding in the packed column.

For the succeeding data, it can be observed that as the water flow rate increases, the loading and flooding points were observed at lower air flow rates. Since the flow inside the column is in countercurrent, the space at which air can flow is reduced as the water flow rate is increased. Since air cannot pass through effectively, accumulation of liquid happens at the base of the column which signifies the loading point. Further increase in the air flow rate causes the accumulation to increase to a point where gas bubbles violently through the liquid at the top of the column which signifies the flooding point. Furthermore, as the water flow rate increases, the difference between the air flow rate at which the loading and flooding point occurred decreases which means that at higher water flow rates, a lesser magnitude of air velocity is needed to reach the flooding point.

3. Loading and flooding curves of the packed column based on the general correlation by Sherwood, Shipley, and Holloway

Sherwood, Shipley and Holloway are one of the early researchers who investigated flow phenomena and were able to propose the first generalized correlation for flooding of packed columns based on tests from air-water systems. The relation is expressed as,

$$\left(\frac{v'^2 a_v \rho_G}{g\varepsilon^3 \rho_L}\right)\mu_L^{\ 0.2} = \frac{L}{G}\sqrt{\frac{\rho_g}{\rho_l}} \qquad [3]$$

where v' is the superficial velocity, a_v is the total area of packing, ρ_G is the density of gas, g is the acceleration due to gravity, ε is the void friction, ρ_L is the density of liquid, L is the liquid mass rate and G is the gas mass rate. The right-hand side of the relation is the dimensionless flow parameter which describes the liquid's kinetic energy relative to the kinetic energy of the gas. The left-hand side of the relation is the capacity parameter which describes the ratio between the kinetic energy of the gas and the potential energy of the liquid multiplied to the viscosity factor (Sherwood et al., 1938).

The suggested method of constructing loading and flooding curves is to plot as abscissa the flow parameter and as ordinate the capacity parameter. Using the graph, the loading and flooding velocities can be obtained for an air-water system with Raschig ring random packings. Given the flow rates, density, and viscosity of the gas and liquid, porosity and diameter of the column, the loading and flooding velocities can be known. It is important to know these quantities since usually these are the limiting values which will dictate the performance of the absorption column. In most industries, it is usually preferred that the optimum flow rate is 50 – 70 % of the flooding velocity (Valenz et al., 2013).

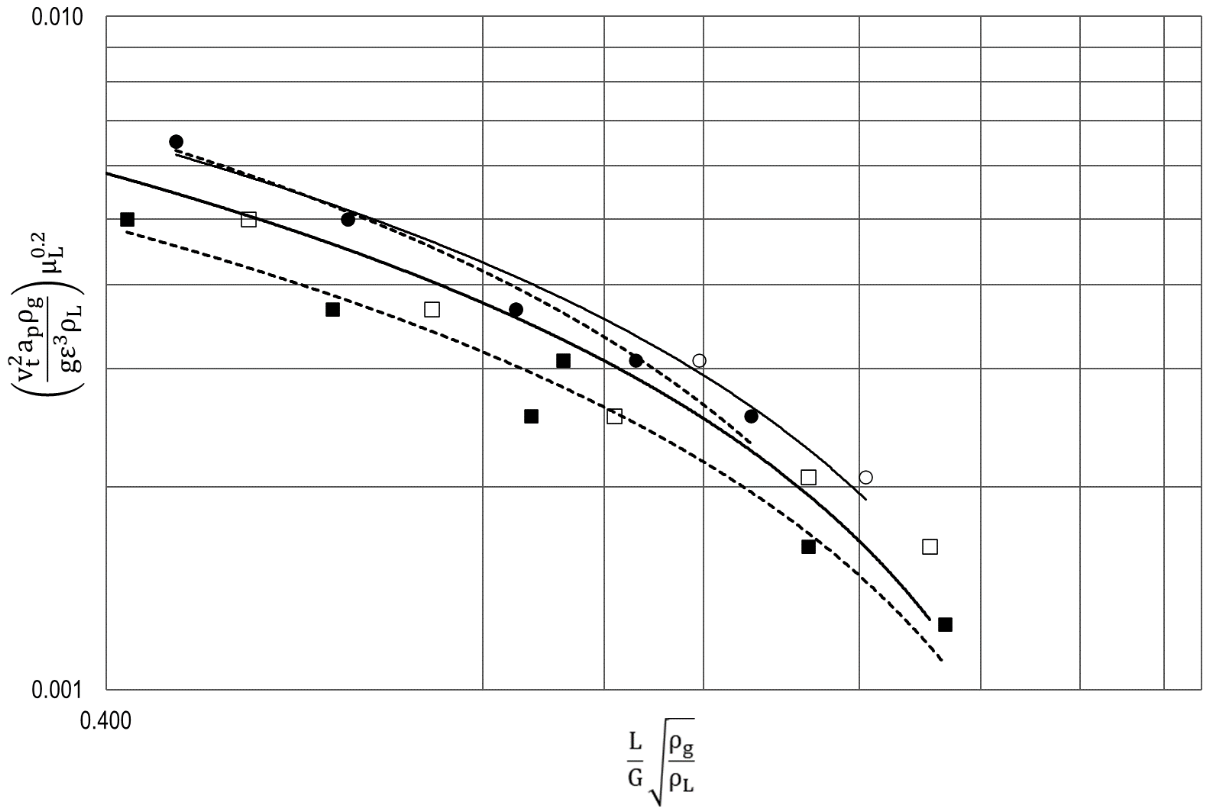

Figure 3. Loading and Flooding Curves of the Packed Column based from the General Correlation by Sherwood, Shipley and Holloway (dashed line and closed symbol: graphical; bold line and open symbol: visual; square: loading point; circle: flooding point)

The area between the loading and flooding curve pertains to the range of operability of the pack column. At this range, the contact between the water and air is sufficient enough to enable efficient mass transfer with respect to the absorbed component. From figure 3, it can be observed that the area between the loading and flooding curve for both graphical and visual decreases in size as the flow parameter increases. This indicates that at higher flow rates, the range of operability of the packed column for effective absorption decreases and the loading and flooding points become undistinguishable.

Moreover, it can be inferred from the graph that as the ratio between the liquid and gas mass flow rate increases, the magnitude of the loading and flooding velocity decreases. This implies that for larger liquid flow rates, lesser magnitude of gas velocity is needed for the column to reach flooding point. This is verified by the tabulated data found in Annex 2 where for both the graphical and visual loading and flooding points; with a higher water flow rate setting, the air velocities at loading point have a closer magnitude with the velocity at flooding point.

From the graph, it can also be observed that the area between the loading and flooding curve is larger in the data determined graphically compared to the data obtained visually. The difference in the data could be a result of a random error since the determination of loading and flooding points using visual observation is subjective which depends on the observer. Flooding can be noted directly because it is defined that as soon as the water starts to accumulate the top part of the packed column rather reaches the top part of the packed column that is flooding; whereas for the case of loading, it can be hardly determined since loading can be very subjective to the eyes of the observer.

Conclusions

The pressure drop across a wet packed absorption column follows a positive relationship with air flow rate. Pressure drop measured experimentally is higher than that of the theoretically calculated pressure drop which may have resulted due to the void spaces that have no packings and due to the wet column that has increased the resistance in the column hence the percent difference between the experimental and theoretical values ranges from 6- 40%.

There is no loading point determined both in visual and graphical methods at 1.5 L/min water flow rate. In water flow rates 2.5, 3.0, 3.5, 4.0, 4.5 L/min, the loading points by visual observation are at air flow rates 160, 140, 120, 100, 90, and 80 L/min, respectively. By graphical method, the loading points are at 140, 120, 100, 110, 80, and 70 L/min, respectively. On the other hand, there were no flooding points determined in both visual and graphical methods at water flow rates 1.5 and 2.0 L/min. In water flow rates 3.0, 3.5, 4.0, 4.5 L/min, the flooding points by visual observation are at air flow rates 160, 140, 120, 110, and 90 L/min, respectively. By graphical method, the flooding points are at 160, 140, 120, 110, and 100 L/min, respectively. The loading and flooding points decrease as the water flow rate increases.

The generated loading and flooding curves based on Sherwood, Shipley, and Holloway correlations can be used to determine the range of operability of the packed column used in the experiment. The extent of the occurrence of an effective mass transfer between the gas and the liquid through absorption can be observed from the area between the generated loading and flooding curves. This also indicates the air velocity requirements that could help achieve the said conditions. It showed that at higher flow rates, the range of operability of the packed column for effective absorption decreases and the loading and flooding points become undistinguishable.

References

Ajibola, B.K. (2010). Optimization of Flooding in an Absorption-Desorption Unit.

Bayram, M., Kayiran, S.N., & Arslan, O. (2018). Application of Ergun's Equation in Food Unit Operations.

Coulson, J. M., Richardson, J. F., Harker, J. H., & Backhurst, J. R. (2002). Coulson and Richardson's Chemical Engineering. Butterworth/Heinemann.

Foust, A. S. (1980). Principles of Unit Operations, 2nd edition. John Wiley & Sons, Inc.

Geankoplis, C. J., Hersel, A., & Lepek, D. J. (2018). Transport Processes and Separation Process Principles. Pearson.

McCabe, W. L., Smith, J. C., & Harriott, P. (2005). Unit Operations of Chemical Engineering. New York: McGraw-Hill Inc.

Sherwood, T., Shipley, G., & Holloway, F. (1938). Flooding Velocities in Packed Columns. Industrial &Amp; Engineering Chemistry, 30(7), 765-769. doi: 10.1021/ie50343a008

Valenz, L., Haidl, J., & Linek, V. (2013). The Effect of Column Diameter and Packing Height on the Pressure Drop and on the HETP of Structured Packings. *Industrial &Amp; Engineering Chemistry Research*, *52*(17), 5967-5974. doi: 10.1021/ie302397q

ANNEX 1: Raw Data Sheets

[Please see attached scanned hard copy of raw data sheets]

Table A1-1. Packed Column Data and Settings

Packed Column Data	
Column Diameter (cm)	7.5
Height (m)	1.46
Packing material used	Raschig Rings
Packing Diameter (mm)	9
Specific Area of Packing ($\frac{m^2}{m^3}$)	420
Percent Void Space (%)	63

Setting				
No.	Manometer Type	Sampling Points		Water Flow Rates for Part C $\left(\frac{L}{min}\right)$
		Part B	Part C	
3	Water	S1 & S2	S1 & S2	1.5, 2, 2.5, 3, 3.5, 4, 4.5

Table A1-2. Pressure Drop in a Wetted Column with Increasing Flow Rates

	Starting Operational Temperature (℃)	Final Operational Temperature (℃)
Gas (Air)	26.0	29.0
Liquid (Water)	28.0	27.0

Air flow rate $\left(\frac{L}{min}\right)$	Height of water in manometer (cm)		
	h_1 (cm)	h_2 (cm)	Δh (cm)
20	0.8	0.6	0.2
40	1.0	0.6	0.4
60	1.0	0.4	0.6
80	1.4	0.2	1.2
100	1.6	-0.2	1.8
130	2.2	-0.8	3.0
140	2.4	-1.0	3.4
150	2.8	-1.2	4.0
160	3.0	-1.4	4.4
170	3.2	-1.6	4.8
Observations: As the air flow rate was increased, the pressure difference reading was also increased.			

Table A1-3. Pressure Drop in a Wetted Column with decreasing flow rates

	Initial Operational Temperature (℃)	Final Operational Temperature (℃)
Gas (Air)	26.0	29.0
Liquid (Water)	28.0	27.0

Air flow rate $\left(\frac{L}{min}\right)$	Height of water in manometer (cm)		
	h_1 (cm)	h_2 (cm)	Δh (cm)
170	3.2	-1.8	5.0
160	3.0	-1.6	4.6
150	2.8	-1.2	4.0
140	2.4	-1.0	3.4
130	2.2	-0.8	3.0
100	1.6	-0.2	1.8
80	1.2	0.0	1.2
60	1.0	0.4	0.6
40	0.8	0.4	0.4
20	0.8	0.6	0.2
Observations: As the air flow rate was decreased, the pressure difference reading from the water manometer was also decreased.			

Table A1-4. Loading and Flooding Points in the Packed Column

	Initial Operational Temperature (℃)	Final Operational Temperature (℃)
Gas (Air)	28.0	28.0
Liquid (Water)	30.0	30.0

Water Flow Rate no.	Water flow rate $\left(\frac{L}{min}\right)$	Air flow rate no.	Air flow rate $\left(\frac{L}{min}\right)$	Height of water in manometer (cm)	
				h_1 (cm)	h_2 (cm)
1	1.5	1	20	0.6	0.6
		2	40	0.8	0.4
		3	60	1.2	0.2
		4	80	1.8	-0.4
		5	100	2.4	-1.0
		6	120	3.0	-1.8
		7	130	3.6	-2.4

Water Flow Rate no.	Water flow rate $\left(\frac{L}{min}\right)$	Air flow rate no.	Air flow rate $\left(\frac{L}{min}\right)$	h_1 (cm)	h_2 (cm)
		8	140	4.0	-2.6
		9	150	4.8	-3.4
		10	160	5.2	-3.8

Observations: As air flow rate increases, the h1 reading increases while the h2 reading decreases. There was no loading and flooding points observed.

Water Flow Rate no.	Water flow rate $\left(\frac{L}{min}\right)$	Air flow rate no.	Air flow rate $\left(\frac{L}{min}\right)$	Height of water in manometer (cm)	
				h_1 (cm)	h_2 (cm)
2	2.0	1	20	0.8	0.6
		2	40	1.0	0.2
		3	60	1.2	0.0
		4	80	1.8	-0.6
		5	90	2.2	-1.0
		6	100	2.6	-1.2
		7	110	3.0	-1.8
		8	120	3.8	-2.6
		9	140	5.0	-3.8
		10	160	7.6	-6.4

Observations: As air flow rate increases, the h1 reading increases while the h2 reading decreases. The loading point can be observed at 160 L/min air flow rate, while no flooding point is observed.

Water Flow Rate no.	Water flow rate $\left(\frac{L}{min}\right)$	Air flow rate no.	Air flow rate $\left(\frac{L}{min}\right)$	Height of water in manometer (cm)	
				h_1 (cm)	h_2 (cm)

3	2.5	1	20	0.8	0.4
		2	40	1.0	0.2
		3	60	1.4	-0.2
		4	80	2.4	-1.2
		5	90	3.0	-1.6
		6	100	3.8	-2.6
		7	110	4.6	-3.4
		8	120	5.4	-4.2
		9	140	8.4	-6.2
		10	160	17.0	-16.0

Observations: As air flow rate increases, the h1 reading increases while the h2 reading decreases. The loading point is at 140 L/min while the flooding point is at 160 L/min.

Water Flow Rate no.	Water flow rate $\left(\frac{L}{min}\right)$	Air flow rate no.	Air flow rate $\left(\frac{L}{min}\right)$	Height of water in manometer (cm)	
				h_1 (cm)	h_2 (cm)
4	3.0	1	20	0.8	0.4
		2	40	1.0	0.0
		3	60	1.6	-0.6
		4	70	2.0	-1.0
		5	80	2.6	-1.6
		6	90	3.4	-2.4
		7	100	4.4	-3.4
		8	110	8.0	-6.8
		9	120	10.0	-9.0

		10	140	18.4	-17.4
Observations: As air flow rate increases, the h1 reading increases while the h2 reading decreases. The loading point can be observed at air flow rate 120 L/min while the flooding point is at 140 L/min.					

Water Flow Rate no.	Water flow rate $\left(\frac{L}{min}\right)$	Air flow rate no.	Air flow rate $\left(\frac{L}{min}\right)$	Height of water in manometer (cm)	
				h_1 (cm)	h_2 (cm)
5	3.5	1	20	0.8	0.4
		2	40	1.2	0.0
		3	50	1.6	-0.4
		4	60	2.0	-0.8
		5	70	2.6	-1.2
		6	80	3.4	-2.2
		7	90	4.4	-3.2
		8	100	5.8	-4.6
		9	110	8.2	-7.0
		10	120	17.2	-16.4
Observations: As air flow rate increases, the h1 reading increases while the h2 reading decreases. The loading point is at 100 L/min air flow rate while the flooding point is at 120 L/min.					

Water Flow Rate no.	Water flow rate $\left(\frac{L}{min}\right)$	Air flow rate no.	Air flow rate $\left(\frac{L}{min}\right)$	Height of water in manometer (cm)	
				h_1 (cm)	h_2 (cm)
6	4.0	1	20	0.8	0.4
		2	30	1.0	0.2

		3	40	1.2	-0.2
		4	50	1.6	-0.4
		5	60	2.4	-1.2
		6	70	3.8	-1.6
		7	80	4.2	-3.8
		8	90	5.4	-4.2
		9	100	7.2	-6.0
		10	110	10.4	-9.2

Observations: As air flow rate increases, the h1 reading increases while the h2 reading decreases. The loading point can be seen at 90 L/min air flow rate while the flooding point can be observed at 110 L/min.

Water Flow Rate no.	Water flow rate $\left(\frac{L}{min}\right)$	Air flow rate no.	Air flow rate $\left(\frac{L}{min}\right)$	Height of water in manometer (cm)	
				h_1 (cm)	h_2 (cm)
7	4.5	1	20	0.8	0.4
		2	30	1.0	0.2
		3	40	1.2	0.0
		4	50	1.6	-0.2
		5	60	2.2	-1.0
		6	70	3.0	-1.6
		7	80	4.8	-3.6
		8	90	6.6	-5.2
		9	100	9.2	-8.0
		10			

Observations: As air flow rate increases, the h1 reading increases while the h2 reading decreases. The loading point can be seen at 80 L/min air flow rate and the flooding point is at 90 L/min.
Overall observation: As water flow rate increases, the air flow rate needed to reach the loading and flooding point decreases. After reaching the loading points, succeeding measurements of h1 increases drastically while h2 decreases drastically when flooding point is reached.

ANNEX 2: Processing of Data

Table A2-1. Equipment specifications and fluid properties

Column	
Column Diameter (D_C), *m*	0.0175
Column Length (ΔL), *m*	0.595
Sampling points	S1 and S2
Packing	
Packing Material	Raschig rings
Packing Diameter (D_P), *m*	0.0027
Specific surface area (a_V), m^{-1}	420
Sphericity (Ψ_S)	0.3
Porosity (ε)	0.63
Liquid	
Type of liquid	Water
Initial Temperature (T), °C	28
Final Temperature (T), °C	27
Viscosity (μ_L), *Pa·s*	0.000842
Density (ρ_L), $kg \cdot m^{-3}$	996.39
Gas	
Type of gas	Air
Initial Temperature (T), °C	26
Final Temperature (T), °C	29
Viscosity (μ_G), *Pa·s*	1.85×10^{-5}
Density (ρ_G), $kg \cdot m^{-3}$	1.174

**Density and Viscosity data are taken from Geankopolis, C. J., Hershel, A. A., & Lepek, D. H. (2018). Transport Processes and Separation Process Principles (4th ed.). United States of America: Pearson Education Inc.*

Sample calculations:

Packing diameter (D_p)

Since the packing material used is Raschig Rings, its sphericity should be considered to get its packing diameter.

$$D_p = \Psi_S\, D_p^* = (0.3)(0.009\ m) = 0.0027\ m \quad \text{[A2-1.1]}$$

Column Length (ΔL)

The sampling points used are S1 and S2; hence, the column length must only be the length of the column from point S1 to S2. Moreover, there is also a void space (no packings) in the columns. This should also be taken into account.

$$\Delta L = \frac{\Delta L^*}{2} - \Delta L_{void} = \frac{1.46\ m}{2} - 0.135\ m = 0.595\ m \qquad \text{[A2-2.2]}$$

Table A2-2. Experimental determination of pressure drop

Air flow rate (q'_G), *L/min*	**Trial 1**				**Trial 2**				**Average Pressure drop (ΔP_{expt}), *Pa***
	Height of water in manometer			**Pressure drop (ΔP_{expt}), *Pa***	**Height of water in manometer**			**Pressure drop (ΔP_{expt}), *Pa***	
	h_1, *cm*	**h_2, *cm***	**Δh, *m***		**h_1, *cm***	**h_2, *cm***	**Δh, *m***		
20	0.8	0.6	0.002	19.55	0.8	0.6	0.002	19.55	19.55
40	1	0.6	0.004	39.10	0.8	0.4	0.004	39.10	39.10
60	1	0.4	0.006	58.65	1	0.4	0.006	58.65	58.65
80	1.4	0.2	0.012	117.30	1.2	0	0.012	117.30	117.30
100	1.6	-0.2	0.018	175.94	1.6	-0.2	0.018	175.94	175.94
130	2.2	-0.8	0.03	293.24	2.2	-0.8	0.03	293.24	293.24
140	2.4	-1	0.034	332.34	2.4	-1	0.034	332.34	332.34
150	2.8	-1.2	0.04	390.98	2.8	-1.2	0.04	390.98	390.98
160	3	-1.4	0.044	430.08	3	-1.6	0.046	449.63	439.86
170	3.2	-1.6	0.048	469.18	3.2	-1.8	0.05	488.73	478.95

Sample calculations:

Air flow rate at 60 L/min

Change in height of water in manometer, Δh

The difference of the height of water in the manometer reading can be obtained using the equation

$$\Delta h = h_1 - h_2 = 1 - 0.4 = 0.6\ cm \quad [A2\text{-}2.1]$$

Experimental pressure drop (ΔP_{expt})

The experimental pressure drop can be determined through the product of the change in height of water in the manometer, the gravitational acceleration, and the density of water.

$$\Delta P_{expt} = \rho_L \Delta h g = \left(996.39 \frac{kg}{m^3}\right)(0.006\ m)\left(9.81 \frac{m}{s}\right) = 58.65\ Pa \quad [A2\text{-}2.2]$$

Table A2-3. Theoretical calculation of pressure drop

Air flow rate (q'$_G$), *L/min*	**Air flow rate (q'$_G$), *m³/s***	**Superficial velocity (v'), *m/s***	**Pressure drop (ΔP_{theo}), *Pa***
20	0.00033	0.08	13.16
40	0.00067	0.15	33.95
60	0.00100	0.23	62.36
80	0.00133	0.30	98.41
100	0.00167	0.38	142.08
130	0.00217	0.49	221.89
140	0.00233	0.53	252.31
150	0.00250	0.57	284.63
160	0.00267	0.60	318.86
170	0.00283	0.64	355.00

Sample calculations:

Air flow rate at 60 L/min

Air flow rate (q'$_G$) in *m^3/s*

The air flow rate (q'$_G$) in m^3/s can be obtained by converting the units of the air flow rate reading from the manometer from L/min to m^3/s using a conversion factor of $1 \frac{L}{min} = \frac{1}{60000} \frac{m^3}{s}$.

$$q'_G = \left(60\frac{L}{min}\right)\left(\frac{\frac{1}{60000}\frac{m^3}{s}}{1\frac{L}{min}}\right) = 0.0010\frac{m^3}{s}$$ [A2-3.1]

Superficial velocity (v')

The superficial velocity (v') can be calculated by dividing the gas flow rate reading from the flowmeter by the cross-sectional area of the column, A_C.

$$v' = \frac{q'_G}{A_C} = \frac{q'_G}{\frac{1}{4}\pi D_C{}^2} = \frac{0.0010\frac{m^3}{s}}{\frac{1}{4}\pi(0.075\ m)^2} = 0.23\frac{m}{s}$$ [A2-3.2]

Theoretical pressure drop (ΔP_{theo})

The theoretical pressure drop, ΔP_{theo} can be estimated using Ergun's equation.

For the laminar term:

$$\Delta P_{theo}(laminar) = \frac{150\mu_G v'\Delta L}{D_p^2}\frac{(1-\varepsilon)^2}{\varepsilon^3} = \frac{150(1.85\times10^{-5})(0.23)(0.595)}{(0.0027)^2}\frac{(1-0.63)^2}{0.63^3} = 28.04\ Pa$$ [A2-3.3]

For turbulent term:

$$\Delta P_{theo}(turbulent) = \frac{1.75\rho_G v'^2\Delta L}{D_p}\frac{(1-\varepsilon)}{\varepsilon^3} = \frac{1.75(1.174)(0.23)^2(0.595)}{0.0027}\frac{(1-0.63)}{0.63^3} = 34.33\ Pa$$ [A2-3.4]

Hence,

$$\Delta P_{theo} = \Delta P_{theo}(laminar) + \Delta P_{theo}(turbulent) = 28.04\ Pa + 34.33\ Pa = 62.36\ Pa$$ [A2-3.45]

Percent difference

A percent difference will be used to quantitatively compare the results of the theoretical and experimental pressure drops.

$$\%diff = \left|\frac{\Delta P_{expt} - \Delta P_{theo}}{\frac{\Delta P_{expt} + \Delta P_{theo}}{2}}\right| \times 100 = \left|\frac{58.65\ Pa - 62.36\ Pa}{\frac{58.65\ Pa + 62.36\ Pa}{2}}\right| \times 100 = 6.14\%$$ [A2-3.5]

Table A2-4. Determination of flooding and loading points through graphical method

Water flow rate (q'_L), *L/min*	Air flow rate no.	Air flow rate (q'_G), *L/min*	Air flow rate (q'_G), m^3/s	Height of water in manometer		Δh, *cm*	Pressure drop per packed column length (ΔP/ΔL), *Pa/m*	Superficial velocity (v'), *m/s*	Gas Mass Rate (G), kg/m^2-s
				h_1, *cm*	h_2, *cm*				
1.5	**1**	20	0.0003	0.6	0.6	0.0	-	0.0755	-
	2	40	0.0007	0.8	0.4	0.4	65.9271	0.1772	0.1769
	3	60	0.0010	1.2	0.2	1	164.8176	0.2657	0.2653
	4	80	0.0013	1.8	-0.4	2.2	362.5988	0.3543	0.3537
	5	100	0.0017	2.4	-1	3.4	560.3800	0.4429	0.4421
	6	120	0.0020	3	-1.8	4.8	791.1247	0.5315	0.5306
	7	130	0.0022	3.6	-2.4	6	988.9059	0.5758	0.5748
	8	140	0.0023	4	-2.6	6.6	1087.7965	0.6201	0.6190
	9	170	0.0028	4.8	-3.4	8.2	1351.5047	0.7529	0.7516
	10	180	0.0030	5.2	-3.8	9	1483.3588	0.7972	0.7959
						0.4			
2.0	**1**	20	0.0003	0.8	0.6	0.2	32.9635	0.0886	0.0884
	2	40	0.0007	1	0.2	0.8	131.8541	0.1772	0.1769
	3	60	0.0010	1.2	0	1.2	197.7812	0.2657	0.2653
	4	80	0.0013	1.8	-0.6	2.4	395.5624	0.3543	0.3537
	5	90	0.0015	2.2	-1	3.2	527.4165	0.3986	0.3979
	6	100	0.0017	2.6	-1.2	3.8	626.3071	0.4429	0.4421
	7	110	0.0018	3	-1.8	4.8	791.1247	0.4872	0.4864
	8	120	0.0020	3.8	-2.6	6.4	1054.8329	0.5315	0.5306
	9	140	0.0023	5	-3.8	8.8	1450.3953	0.6201	0.6190
	10	160	0.0027	7.6	-6.4	14	2307.4471	0.7086	0.7074
2.5	**1**	20	0.0003	0.8	0.4	0.4	65.9271	0.0886	0.0884
	2	40	0.0007	1	0.2	0.8	131.8541	0.1772	0.1769
	3	60	0.0010	1.4	-0.2	1.6	263.7082	0.2657	0.2653
	4	80	0.0013	2.4	-1.2	3.6	593.3435	0.3543	0.3537
	5	90	0.0015	3	-1.6	4.6	758.1612	0.3986	0.3979
	6	100	0.0017	3.8	-2.6	6.4	1054.8329	0.4429	0.4421
	7	110	0.0018	4.6	-3.4	8	1318.5412	0.4872	0.4864
	8	120	0.0020	5.4	-4.2	9.6	1582.2494	0.5315	0.5306
	9	140	0.0023	8.4	-6.2	14.6	2406.3376	0.6201	0.6190
	10	160	0.0027	17	-16	33	5421.1989	0.7086	0.7086
3.0	**1**	20	0.0003	0.8	0.4	0.4	65.9271	0.0886	0.1769
	2	40	0.0007	1	0	1	164.8176	0.1772	0.2653
	3	60	0.0010	1.6	-0.6	2.2	362.5988	0.2657	0.3095
	4	70	0.0012	2	-1	3	494.4529	0.3100	0.3537
	5	80	0.0013	2.6	-1.6	4.2	692.2341	0.3543	0.3979
	6	90	0.0015	3.4	-2.4	5.8	955.9424	0.3986	0.4421
	7	100	0.0017	4.4	-3.4	7.8	1285.5776	0.4429	0.4864

	8	110	0.0018	8	-6.8	14.8	2439.3012	0.4872	0.5306
	9	120	0.0020	10	-9	19	3131.5353	0.5315	0.6190
	10	140	0.0023	18.4	-17.4	35.8	5900.4718	0.6201	0.0884
3.5	**1**	20	0.0003	0.8	0.4	0.4	65.9271	0.0886	0.0884
	2	40	0.0007	1.2	0	1.2	197.7812	0.1772	0.1769
	3	50	0.0008	1.6	-0.4	2	329.6353	0.2214	0.2211
	4	60	0.0010	2	-0.8	2.8	461.4894	0.2657	0.2653
	5	70	0.0012	2.6	-1.2	3.8	626.3071	0.3100	0.3095
	6	80	0.0013	3.4	-2.2	5.6	922.9788	0.3543	0.3537
	7	90	0.0015	4.4	-3.2	7.6	1252.6141	0.3986	0.3979
	8	100	0.0017	5.8	-4.6	10.4	1714.1035	0.4429	0.4421
	9	110	0.0018	8.2	-7	15.2	2505.2282	0.4872	0.4864
	10	120	0.0020	17.2	-16.4	33.6	5537.8729	0.5315	0.5306
4.0	**1**	20	0.0003	0.8	0.4	0.4	65.9271	0.0886	0.0884
	2	30	0.0005	1	0.2	0.8	131.8541	0.1329	0.1326
	3	40	0.0007	1.2	-0.2	1.4	230.7447	0.1772	0.1769
	4	50	0.0008	1.6	-0.4	2	329.6353	0.2214	0.2211
	5	60	0.0010	2.4	-1.2	3.6	593.3435	0.2657	0.2653
	6	70	0.0012	3.8	-1.6	5.4	890.0153	0.3100	0.3095
	7	80	0.0013	4.2	-3.8	8	1318.5412	0.3543	0.3537
	8	90	0.0015	5.4	-4.2	9.6	1582.2494	0.3986	0.3979
	9	100	0.0017	7.2	-6	13.2	2175.5929	0.4429	0.4421
	10	110	0.0018	10.4	-9.2	19.6	3230.4259	0.4872	0.4864
4.5	**1**	20	0.0003	0.8	0.4	0.4	65.9271	0.0886	0.0884
	2	30	0.0005	1	0.2	0.8	131.8541	0.1329	0.1326
	3	40	0.0007	1.2	0	1.2	197.7812	0.1772	0.1769
	4	50	0.0008	1.6	-0.2	1.8	296.6718	0.2214	0.2211
	5	60	0.0010	2.2	-1	3.2	527.4165	0.2657	0.2653
	6	70	0.0012	3	-1.6	4.6	758.1612	0.3100	0.3095
	7	80	0.0013	4.8	-3.6	8.4	1384.4682	0.3543	0.3537
	8	90	0.0015	6.6	-5.2	11.8	1944.8482	0.3986	0.3979
	9	100	0.0017	9.2	-8	17.2	2834.8635	0.4429	0.4421

**Highlighted in Yellow is the loading point; Gray is the flooding point. These are determined visually.*

Sample calculations:

Water flow rate at 2.5 L/min; air flow rate at 160 L/min

Change in height of water in manometer, Δh

The same equation is used in determining the difference of the height of water in the manometer reading. Refer to equation A2-2.1.

Air flow rate (q'_G) in m^3/s

The same set of equation from the conversion of air flow rate units from L/min to m^3/s. Refer to equation A2-3.1.

Superficial velocity (v')

The same equation is used in determining the superficial velocity. Refer to equation A2-3.2.

Pressure drop per packed column length (ΔP/ΔL)

The pressure drop per packed column length can be determined by dividing the experimental pressure drop to the length of the packed column.

$$\frac{\Delta P}{\Delta L} = \frac{\rho_L \Delta hg}{\Delta L} = \frac{\left(996.39\frac{kg}{m^3}\right)(33\ cm)\left(\frac{1\ m}{100\ cm}\right)\left(9.81\frac{m}{s}\right)}{0.595} = 5421.20\ \frac{Pa}{m} \quad \text{[A2-4.1]}$$

Gas Mass Rate (G)

The Gas Mass Rate, *G* can be calculated by multiplying the air flow rate in m^3/s to the density of gas divided by the column's cross-sectional area.

$$G = \frac{q'_G \rho_G}{A_C} = \frac{\left(0.0026667\frac{m^3}{s}\right)\left(1.174\frac{kg}{m^3}\right)}{0.004418\ m^2} = 0.7086\frac{kg}{m^2 s} \quad \text{[A2-4.2]}$$

Flooding and Loading Points

The pressure drop across the column with at least 10 appropriate air flowrates for 7 different water flow rates is determined. A plot of $(\frac{\Delta P}{\Delta L})$ vs G in a log-log graph for each water flowrate is constructed. Note that $(\frac{\Delta P}{\Delta L})$ is the pressure drop per meter of packing. The loading point and flooding point are determined by identifying the inflection points of the pressure drop curve. Specifically, the loading point is the point at which there is a drastic change in the slope of the pressure drop line. While the flooding point is the point at which the pressure drop curve is vertical or nearly so at this point (its slope approaches infinity). A step-by-step procedure on the graphical determination of the loading and flooding points is listed below:

- Draw three lines that best fit the points on the graph generated. The slopes of the lines must be significantly different, such that the first line best fit the first point until the point where a second-best fit line must be drawn, and another (and third) line of best fit is drawn for the last two or three point on the graph (this line may be nearly vertical).
- Mark the intersections of these three lines. (a) point 1 for the intersection of lines 1 and 2; and (b) point 2 for the intersection of lines 2 and 3.
- The first intersection will be the loading point and the second intersection is the flooding point.

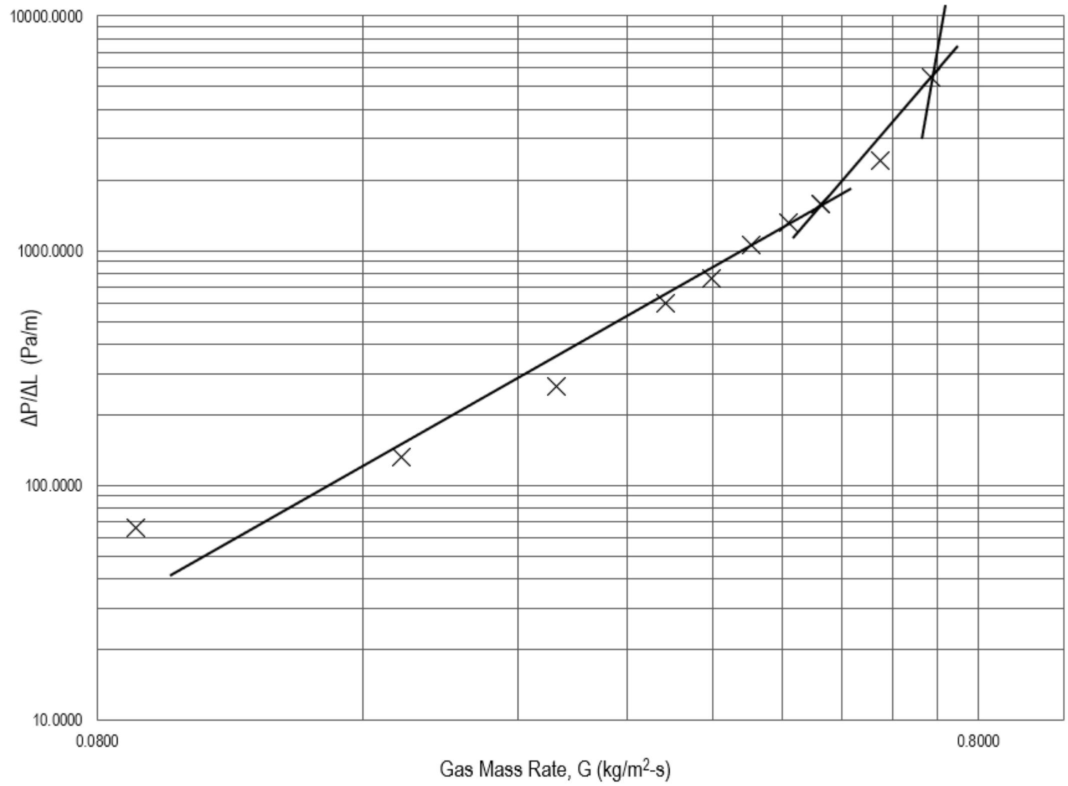

Figure A2-4. Graphical determination of loading and flooding points

Table A2-5. Data needed for construction of flooding curves of experimental data of the packed column based on the generalized correlations proposed by Sherwood, Shipley, and Holloway (1938).

Water flow rate (q'_L), *L/min*	Water flow rate (q'_L), *m^3/s*	Liquid Mass Rate (L), *kg/m^2-s*	Flooding					
			Air flow rate (q'_G), *L/min*	Air flow rate (q'_G), *m^3/s*	Gas Mass Rate (G), kg/m^2-s	Superficial velocity (v'), *m/s*	$\frac{L}{G}\sqrt{\frac{\rho_g}{\rho_L}}$	$\left(\frac{v'^2 a_p \rho_g}{g\varepsilon^3\rho_L}\right)\mu_L^{0.2}$
1.500	0.00002500	5.634	No flooding occurs					
2.000	0.00003333	7.512	No flooding occurs					
2.500	0.00004167	9.390	160.000	0.003	0.709	0.604	0.4809	0.007
3.000	0.00005000	11.268	140.000	0.002	0.620	0.528	0.624	0.005
3.500	0.00005833	13.146	120.000	0.002	0.531	0.453	0.849	0.004
4.500	0.00007500	16.902	110.000	0.002	0.487	0.415	1.191	0.003
5.000	0.00008333	18.780	90.000	0.002	0.399	0.340	1.618	0.002
Water flow rate (q'_L), *L/min*	**Water flow rate (q'_L), *m^3/s***	**Liquid Mass Rate (L), *kg-/m^2-s***	**Loading**					
			Air flow rate (q'_G), *L/min*	**Air flow rate (q'_G), *m^3/s***	**Gas Mass Rate (G), kg-/m^2-s**	**Superficial velocity (v'), *m/s***	$\frac{L}{G}\sqrt{\frac{\rho_g}{\rho_L}}$	$\left(\frac{v'^2 a_p \rho_g}{g\varepsilon^3\rho_L}\right)\mu_L^{0.2}$
1.500	0.00002500	5.634	No loading occurs					
2.000	0.00003333	7.512	160.000	0.003	0.709	0.604	0.364	0.007
2.500	0.00004167	9.932	140.000	0.002	0.620	0.528	0.520	0.005
3.000	0.00005000	11.268	120.000	0.002	0.531	0.453	0.728	0.004
3.500	0.00005833	13.146	100.000	0.002	0.443	0.377	1.019	0.003
4.500	0.00007500	16.902	90.000	0.002	0.399	0.340	1.456	0.002
5.000	0.00008333	18.780	80.000	0.001	0.354	0.302	1.820	0.002

Sample calculations:

Water flow rate at 2.5 L/min; flooding

Air flow rate (q'_G) in *m^3/s*

The same set of equation from the conversion of air flow rate units from L/min to m^3/s. Refer to equation A2-3.1.

Superficial velocity (v')

The same equation is used in determining the superficial velocity. Refer to equation A2-3.2.

Gas Mass Rate (G)

The same equation is used in determining the Gas Mass Rate. Refer to equation A2-4.2.

Liquid Mass Rate (L)

The Liquid Mass Rate, *L* can be calculated by multiplying the water flow rate in m^3/s to the density of water divided by the column's cross-sectional area.

$$G = \frac{q'_L \rho_L}{A_C} = \frac{\left(0.00004167\,\frac{m^3}{s}\right)\left(996.39\,\frac{kg}{m^3}\right)}{0.004418\,m^2} = 9.932\,\frac{kg}{m^2 s}$$ [A2-5.1]

Flow Parameter

The flow parameter can be calculated using a non-dimensional equation which is $\frac{L}{G}\sqrt{\frac{\rho_g}{\rho_L}}$.

$$\frac{L}{G}\sqrt{\frac{\rho_g}{\rho_L}} = \frac{9.932\,\frac{kg}{m^2 s}}{0.709\,\frac{kg}{m^2 s}}\sqrt{\frac{1.174\,\frac{kg}{m^3}}{996.39\,\frac{kg}{m^3}}} = 7.9681997 \times 0.175 = 0.4809$$ [A2-5.2]

Capacity Parameter

The capacity parameter can be calculated using the equation which is $\left(\frac{v_t^2 a_p \rho_g}{g\varepsilon^3 \rho_L}\right)\mu_L^{0.2}$

$$\left(\frac{v'^2 a_p \rho_g}{g\varepsilon^3 \rho_L}\right)\mu_L^{0.2} = \left(\frac{\left(0.604\,\frac{m}{s}\right)^2 \left(420\,m^{-1} \times (1-0.63)\right)\left(1.174\,\frac{kg}{m^3}\right)}{\left(9.81\,\frac{m}{s^2}\right)(0.63)^3\left(996.39\,\frac{kg}{m^3}\right)}\right)(0.000842)^{0.2} = 0.007$$ [A2-5.3]

Constructing loading and flooding curves of the packed column

Loading and flooding curves of the packed column can be constructed from experimental data based on the generalized correlations proposed by Sherwood, Shipley, and Holloway. Plot $\left(\frac{v'^2 a_p \rho_g}{g\varepsilon^3 \rho_L}\right)\mu_L^{0.2}$ vs $\frac{L}{G}\sqrt{\frac{\rho_g}{\rho_L}}$ in a log-log graph to obtain a correlation for estimating flooding at given liquid to gas rates. Presented in Tables A2-5 are the numerical values, from loading and flooding velocities determined by visual method needed for the said generalized correlation.

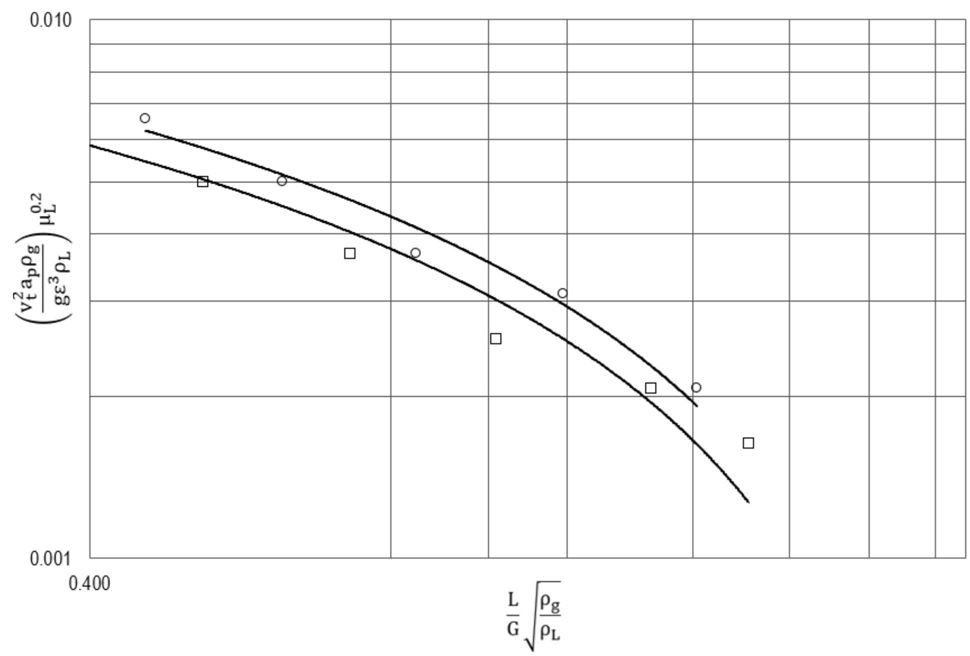

Figure A2-5. Loading and Flooding Curves constructed based on the generalized correlations proposed by Sherwood, Shipley, and Holloway (1938).

GROUP 6
OHLIANN KIRK D. ILLAGA
JEROLD J. MONSANTO
JEAN MERCY C. ROSAL

Raw Data Sheets

Table 1. Packed Column Data and Settings

Column Diameter (cm)	7.5
Height (m)	1.46
Packing Material Used	Raschig Rings
Packing Diameter (mm)	9
Specific Area of Packing ($\frac{m^2}{m^3}$)	420
Percent Void Space (%)	63

Settings:

No.	Manometer Type	Sampling Points		Water Flow rates for Part C
		Part B	Part C	
3	Water	S1 & S2	S1 & S2	1.5, 2, 2.5, 3, 3.5, 4, 4.5

Table 2.1 Pressure Drop in a Wetted Column (From Low to High Flowrate) - Group 5

Liquid (water)	Starting operational temperature (°C):	28
	Final operational temperature (°C)	27
Gas (Air)	Starting operational temperature (°C):	26
	Final operational temperature (°C):	29
Airflow rate $\left(\frac{L}{min}\right)$	**Manometer Reading, pressure difference (cm)**	
20	0.8 - 0.6	0.2
40	1.0 - 0.6	0.4

60	1.0 - 0.4	0.6
80	1.4 - 0.2	1.2
100	1.6 - (-0.2)	1.8
130	2.2 - (-0.8)	3.0
140	2.4 - (-1)	3.4
150	2.8 - (-1.2)	4.0
160	3.0 - (-1.4)	4.4
170	3.2 - (-1.6)	4.8

Observations:

As the air flowrate was increased, the pressure difference (cm) reading from the water mano meter was also increased.

Table 2.2 Pressure Drop in a Wetted Column (From High to Low Flowrate)

Liquid (water)	**Starting operational temperature (°C):**	28
	Final operational temperature (°C)	27
Gas (Air)	**Starting operational temperature (°C):**	26
	Final operational temperature (°C):	29
Airflow rate $\left(\frac{L}{min}\right)$	**Manometer Reading, pressure difference (cm)**	
170	3.2 - (-1.8)	5.0
160	3.0 - (-1.6)	4.6

150	2.8-(-1.2)	4.0
140	2.4 - (-1)	3.4
130	2.2 - (-0.8)	3.0
100	1.6 - (-0.2)	1.8
80	1.2 - 0	1.2
60	1.0 - 0.4	0.6
40	0.8 - 0.4	0.4
20	0.8 - 0.6	0.2
Observations: As the air flowrate was decreased, the pressure difference (cm) reading from the water manometer also decreased.		

Table 3. Determination of Loading and Flooding Point

Liquid Phase Temperature	Initial (°C):	28.0 °C	Sampling Point	S_1
	Final (°C):	28.0°C		
Gas Phase Temperature	Initial (°C):	30.0°C		S_2
	Final (°C):	30.0°C		
Water Flow Rate $\left(\frac{L}{min}\right)$	Air Flow Rate $\left(\frac{L}{min}\right)$	Manometer Reading		Observation
		h_1 (cm)	h_2 (cm)	
1.5	20	~~3~~ 0.6	0.6	- As air flow rate increases, h_1 reading increases
	40	0.8	0.4	
	60	1.2	0.2	

1.5	80	1.8	-0.4	while h_2 reading decreases. - No loading point - No Flooding point
	100	~~1.2~~ 2.4	-1.0	
	120	3.0	-1.8	
	140	4.0	-2.6	
	~~145~~ 150	4.8	-3.4	
	160	5.2	-3.8	
	130	3.6	-2.4	
2	20	0.8	~~0.4~~ 0.6	- As air flow rate increases, h_1 reading also increases while h_2 reading decreases. - Loading point at 160 L/min air flow rate. - No Flooding point
	40	1.0	0.2	
	60	1.2	0	
	80	1.8	-0.6	
	90	2.2	-1.0	
	100	2.6	-1.2	
	110	3.0	-1.8	
	120	3.8	-2.6	
	140	5.0	-3.8	
	160	7.6	-6.4	
2.5	20	0.8	0.4	- As air flow rate increases, h_1 reading also increases while h_2 reading decreases - Loading point at 140 L/min air flowrate - Flooding point at 160 L/min air flow rate.
	40	~~1.2~~ 1.0	0.2	
	60	1.4	-0.2	
	80	2.4	-1.2	
	90	3.0	-1.6	
	100	3.8	-2.6	
	110	4.6	-3.4	
	120	5.4	-4.2	

	140	~~8.2~~ 8.4	-6.2	
	☆ 160	17	-16.0	
3	20	0.8	0.4	- As air flowrate increases, h1 reading also increases while h2 reading decreases - Loading point at 110 L/min air flowrate. - Flooding point at 140 L/min air flowrate.
	40	1.0	0	
	60	1.6	-0.6	
	70	2.0	-1.0	
	80	2.6	-1.6	
	90	3.4	-2.4	
	100	4.4	-3.4	
	110	8.0	-6.8	
	120	10.0	-9.0	
	☆ 140	18.4	-17.4	
3.5	20	0.8	0.4	- As air flowrate increases, h1 reading also increases while h2 reading decreases. - Loading point at 100 L/min air flowrate. - Flooding point at 120 L/min air flowrate.
	40	1.2	0.	
	50	1.6	-0.4	
	60	2.0	-0.8	
	70	2.6	-1.2	
	80	3.4	-2.2	
	90	4.4	-3.2	
	100	5.8	-4.6	
	110	8.2	-7.0	
	☆ 120	17.2	-16.4	
4	20	0.8	0.4	- As air flowrate increases, h1 reading also increases while
	30	1.0	0.2	
	40	1.2	-0.2	

4.	50	1.6	-0.4	h_2 reading decreases. - Loading point at 90 L/min air flowrate -Flooding point at 110 L/min air flowrate.
	60	2.4	-1.2	
	70	3.0	-1.6	
	80	4.2	-3.0	
	90 ✓	5.4	-4.2	
	100	7.2	-6.0	
	☆ 110	10.4	-9.2	
4.5	20	0.8	0.4	- As air flowrate increases, h_1 reading also increases while h_2 reading decreases. - Loading point at 80 L/min air flowrate. - Flooding point at 90 L/min air flowrate.
	30	1.0	0.2	
	40	1.2	0	
	50	1.6	-0.2	
	60	2.2	-1.0	
	70	3.0	-1.8	
	80 ✓	4.8	-3.6	
	90	6.6	-5.2	
	☆ 100	9.2	-8.0	

Observation:

As water flow rate increases, the air flow rate needed to reach loading and flooding point decreases. ~~As water flow rate increases,~~ After reaching the loading point, succeeding measurements of h_1 increases drastically while h_2 decreases drastically. Until flooding point is reached.

04/20/2022